communications biology

A Nature Portfolio journal

Article

https://doi.org/10.1038/s42003-025-07803-8

Nematode serine protease inhibitor SPI-I8 negatively regulates host NF-κB signalling by hijacking MKRN1-mediated polyubiquitination of RACK1

Fei Wu[1,2,6], Yanqiong Chen[1,6], Xueqiu Chen[1], Danni Tong[1], Jingru Zhou[1,3], Zhendong Du[1], Chaoqun Yao[4], Yi Yang[1], Aifang Du[1] & Guangxu Ma[1,5]

Parasitic roundworms are remarkable for their ability to manipulate host immune systems and ameliorate inflammatory diseases. Although much is known about the nature of nematode effectors in immune modulation, little is known about the action mode of these molecules. Here, we report that a serine protease inhibitor SPI-I8 in the extracellular vesicles of blood-feeding nematodes like *Ancylostoma ceylanicum*, *Haemonchus contortus* and *Nippostrongylus brasiliensis*, effectively halts excessive inflammatory responses in vitro and in vivo. We demonstrate that *H. contortus* SPI-I8 promotes the role of a negative regulator of RACK1 and enhances the effects of RACK1 on tumor necrosis factor (TNF)-α–IκB kinases (IKKs)–nuclear factor kappa beta (NF-κB) axis in mammalian cells, by hijacking E3 ubiquitin protein ligase MKRN1-mediated polyubiquitination of RACK1. Administration of recombinant *N. brasiliensis* SPI-I8 effectively protects mice from dextran sulfate sodium (DSS)-induced colitis and lipopolysaccharide (LPS)-induced sepsis. Considering the structural and functional conservation of SPI-I8s among Strongylida nematodes and the conservation of interactive mediators (i.e., MKRN1 and RACK1) among mammals, our findings provide insights into the host-parasite interface where parasitic roundworms secret molecules to suppress host inflammatory responses. Harnessing these findings should underpin the exploitation of nematode's immunomodulators to relief excessive inflammation associated diseases in animals and humans.

Inflammation is often provoked by tissue damage or infection, clinically manifests by swelling, redness, heat and/or pain, and is characterised by the recruitment of leukocytes and soluble proteins[1–3]. In this cellular process, pattern recognition receptors, such as transmembrane toll-like receptors (TLRs) and intracellular nucleotide-binding oligomerisation domain (NOD)-like receptors (NLRs), activate the mitogen-activated protein kinase (MAPK) and nuclear factor kappa beta (NF-κB) signalling pathways, inducing the expression of pro-inflammatory mediators (e.g., interleukins IL-1β and IL-18) to initiate inflammation and associated immune responses[4–7]. Infectious agents, such as viruses, bacteria, fungi and parasites, are known to induce inflammatory and associated immune responses that may lead to immunopathological disorders, such as rheumatoid arthritis, inflammatory bowel disease, diabetes and/or heart disease[8–11]. However, on the other hand, some pathogens, such as parasitic nematodes, have been reported to suppress such responses, leading a resolution or cure of such immunopathological diseases[12–18].

In a physiological state, a body's ability to prevent excessive inflammatory responses requires a rigorous control of pro-inflammatory processes, for instance, via a negative regulation of NF-κB signalling and the NLRP3 inflammasome[19,20]. Various molecules have been described that negatively regulate NF-κB signalling and the NLRP3 inflammasome[21–26]. For example, the receptor for activated C kinase 1 (RACK1, also known as

[1]Institute of Preventive Veterinary Medicine, Zhejiang Provincial Key Laboratory of Preventive Veterinary Medicine, College of Animal Sciences, Zhejiang University, Hangzhou, Zhejiang, China. [2]College of Veterinary Medicine, Anhui Agricultural University, Hefei, China. [3]MOE Frontier Science Center for Brain and Brain-machine integration, Zhejiang University, Hangzhou, Zhejiang, China. [4]Ross University School of Veterinary Medicine and One Health Center for Zoonoses and Tropical Veterinary Medicine, Ross University School of Veterinary Medicine, Basseterre, St. Kitts, Trinidad and Tobago. [5]ZJU-Xinchang Joint Innovation Centre (TianMu Laboratory), Gaochuang Hi-Tech Park, Xinchang, China. [6]These authors contributed equally: Fei Wu, Yanqiong Chen. e-mail: gxma1@zju.edu.cn

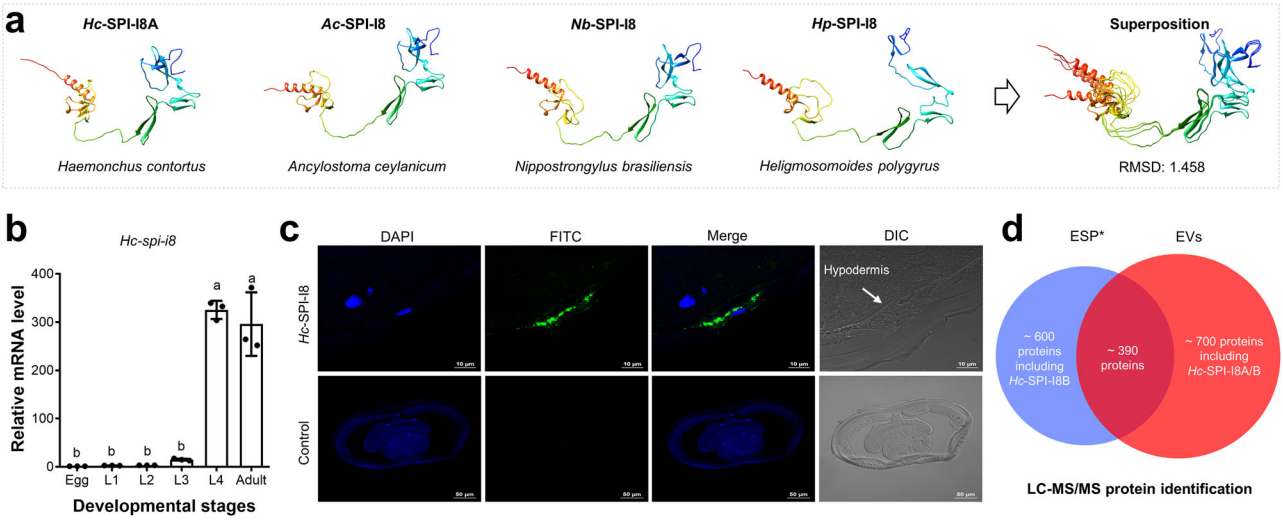

Fig. 1 | Serine protease inhibitor (SPI) I8 is conserved in nematodes of animals. **a** Structures of SPI-I8 orthologs identified in blood-feeding *Haemonchus contortus*, *Ancylostoma ceylanicum* and *Nippostrongylus brasiliensis* and non-blood-feeding *Heligmosomoides polygyrus* are modelled and superimposed for similarity analysis. The sequences of SPI-I8 in nematodes were retrieved from WormBase ParaSite (WBPS18). The structures of the nematode SPI-I8s were modelled using the program AlphaFold2 (v. 2.1.0) and visualised with UCSF ChimeraX (v.1.0). Root-mean-square deviation (RMSD) scores are indicated. **b** Transcriptional profiling of serine protease inhibitor I8 coding gene (*Hc-spi-i8*) among the egg, first- (L1), second (L2), third- (L3), fourth-larval (L4), and adult stages of *Haemonchus contortus*. One-way variance analysis is used to indicate the significance of differential gene transcription among stages. Different letters indicate significance $p < 0.05$. **c** Using a polyclonal antibodies-based immunohistochemistry assay, SPI-I8 is localised to the inner membrane of hypodermis (indicated by white arrow) of female adult *H. contortus*. Mouse anti-Hc-SPI-I8A/ASA polyclonal antibody and pre-immunized mouse sera (control) were used as primer antibodies. Scar bars are 10 or 50 µm. DAPI 4',6-diamidino- 2-phenylindole, FITC fluorescein 5-isothiocyanate, DIC Differential interference contrast microscopy. **d** Detection of SPI-I8 (isoform A/B) in the extracellular vesicles (EVs) and EVs-depleted excretory/secretory products (ESP*) released by the parasitic stages of *H. contortus*, using liquid chromatography–tandem mass spectrometry method. Number of proteins identified in EVs and/or ESP* is indicated.

guanine nucleotide-binding protein subunit beta-2-like 1) can inhibit tumor necrosis factor (TNF)-triggered inflammation by interfering the activation of IκB kinase (IKK complex, the core element of the NF-κB cascade)[27], and G protein subunit β 1 (GNB1) negatively regulates NLRP3 inflammasome activation[25]. Finding a way of reducing inflammation via specific targets in these processes or pathways could lead to new therapies against immunopathological disorders.

Many parasitic worms (e.g., roundworms and flatworms) are masters at maintaining a relatively long-term relationship with their mammalian hosts by modulating/suppressing inflammatory/immune responses via molecules in their excretory/secretory (ES) products or associated extracellular vesicles[28–31]. For instance, some soluble molecules released by parasitic nematodes (i.e. anti-inflammatory protein (AIP)-1 and TGF-β mimic (TGM)-1 from hookworms; *Ts*-serpin from pork worm) can suppress intestinal epithelial tuft cell induction in vitro or treat experimental colitis in vivo in mice[32–37]. However, there is limited understanding of how these worms achieve this balanced relationship (parasitism) without causing acute disease or exacerbating inflammatory/immune responses[38,39]. Indeed, little is known about whether and, if so, precisely how parasitic nematodes negatively regulate inflammation in most host animals and humans.

Recently, we elucidated that serine protease inhibitor I8 (SPI-I8) of a blood-feeding nematode *Haemonchus contortus* inhibits blood coagulation in vitro by interacting with host thrombospondin type-1 (TSP1) domain-containing protein[40]. As this protease inhibitor was shown also interact with other host proteins, including the inflammatory regulation associated protein RACK1, we hypothesised that this nematode SPI-I8 plays a key role in modulating host inflammatory and immune responses. Here, we test this hypothesis.

Results

SPI-I8 orthologs are conserved in Strongylida nematodes

First, we predicted SPI-I8 orthologs in major parasitic nematodes of animals, and candidates were predominantly related to Strongylida nematodes, including *H. contortus* (barber's pole worm), *Ancylostoma ceylanicum* (hookworm of dogs, cats, and humans), *Heligmosomoides polygyrus* and *Nippostrongylus brasiliensis* (hookworm of mice) (Supplementary Table 1). Two distinct isoforms (A = canonical, and B = non-canonical) of SPI-I8 were identified in *H. contortus*[40]. No isoforms of SPI-I8 were predicted in other parasitic nematodes. We showed sequence and structural conservations of those predicted SPI-I8 orthologs (overall root-mean-square deviation: 1.46; Fig. 1a), which suggested a common immunobiological role for this protein in these parasites. By contrast, no orthologs of SPI-I8 were predicted in clade I, III, or IV nematodes of animals. Our attention turned to *H. contortus* as a parasite model because it is a highly significant animal pathogen and because of the extensive resources available for in-depth molecular studies[41–46].

Nematode SPI-I8 is abundantly transcribed and expressed in parasitic stages

For *H. contortus*, we demonstrated that SPI-I8 gene is significantly upregulated in blood-feeding stages (i.e., both L4 and adult) compared with free-living stages (i.e., egg, L1, L2 and L3; $p < 0.0001$; Fig. 1b), in accordance with its protein expression pattern during the life history of this parasite[47]. Using a polyclonal antibodies-based immunofluorescent histochemistry microscopy, SPI-I8A/B was specifically localised to the inner plasma membrane of the hypodermis and associated with excretory cells in both adult female and male worms (Fig. 1c). Both isoforms of SPI-I8 were detected in the extracellular vesicles (EVs) released by *H. contortus*, and SPI-I8B was also detected in the EVs depleted excretory/secretory products (ESP) from the worm (Fig. 1d). These findings suggest that both isoforms of SPI-I8 play a role in parasite-host interactions, including immunity and inflammation. Indeed, we discovered a specific anti-SPI-I8 serum antibody response at 10 days after experimental oral infection of the permissive host (sheep) with *H. contortus*.

Nematode SPI-I8 interacts with host MKRN1 and RACK1

Immunoprecipitation-mass spectrometry (IP-MS) revealed 537 proteins from the stomach (abomasum) wall including epithelium, of sheep

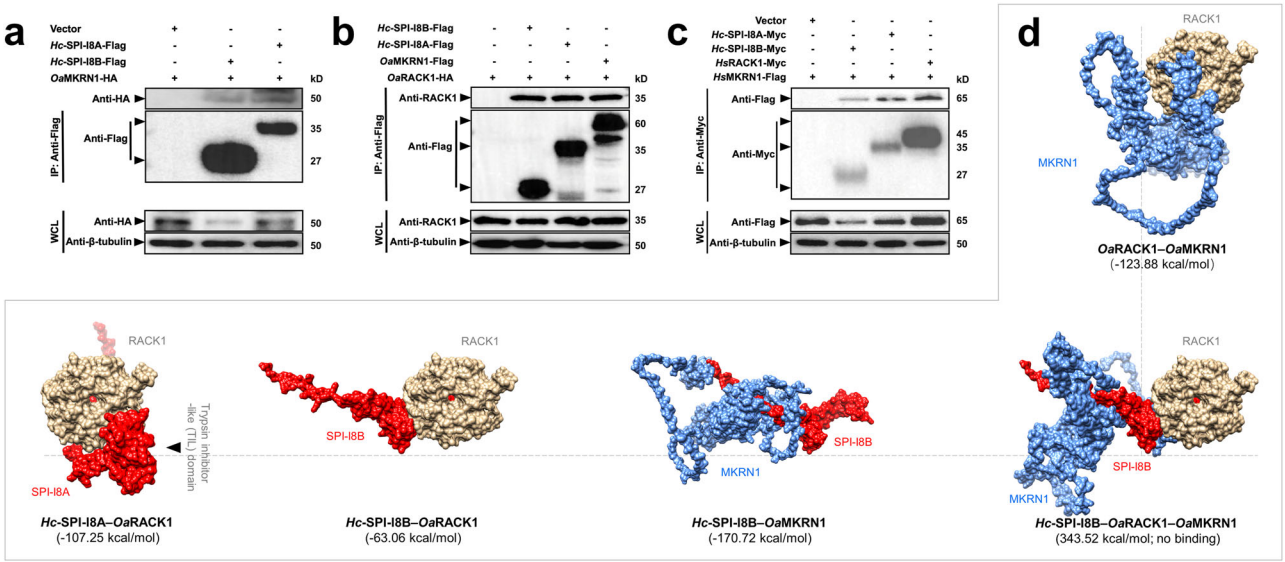

Fig. 2 | Interactions between nematode serine protease inhibitor I8 (SPI-I8) with host proteins. a, **b** Co-immunoprecipitation analysis of Flag-fused *Haemonchus contortus* SPI-I8A/B with HA-fused ovine E3 ubiquitin-protein ligase makorin-1 (*Oa*MKRN1) and/or ovine receptor of activated protein C kinase 1 (*Oa*RACK1) in human embryo kidney (HEK) 293 T cells. **c** Co-immunoprecipitation analysis of Flag-fused human MKRN1 (*Hs*MKRN1) and Myc-fused RACK1 (*Hs*RACK1) in HEK 293 T cells. WCL, whole cell lysate; IP, immunoprecipitated protein. Beta-tubulin is used as the internal control. **d** Molecular docking of *Oa*RACK1 and *Oa*MKRN1, *Hc*-SPI-I8A and *Oa*RACK1, *Hc*-SPI-I8B and *Oa*RACK1, *Hc*-SPI-I8B and *Oa*MKRN1, *Hc*-SPI-I8B, *Oa*RACK1 and *Oa*MKRN1 in silico. It is predicted that the binding of *Hc*-SPI-I8A/B and *Oa*MKRN1 hijacks the space for *Oa*MKRN1 to bind RACK1. *Hc*-SPI-I8A/B is coloured in red, ovine MKRN1 in blue, and *Oa*RACK1 in gold. Binding free energy (ΔG) of each docking was attached. Structures of *Hc*-SPI-I8A/B, the ovine MKRN1 were modelled with AlphaFold2 (v. 2.1.085), and ovine RACK1 retrieved from AlphaFold Protein Structure Database. Molecular docking of molecules was performed using the ClusPro and HawkDock server. Models were displayed and superimposed using UCSF ChimeraX.

(*Ovis aries*). Additionally, yeast cDNA library screening identified more than 200 proteins from ovine peripheral blood mononuclear cells (PBMCs) that interacted with *Hc*-SPI-I8A (Supplementary Fig. 1a, b; Supplementary Table 2). A detailed analysis using pairwise yeast two-hybrid verified seven molecules (Supplementary Table 3). Co-localisation and pull-down assays further revealed that *Hc*-SPI-I8A/B interact specifically with sheep E3 ubiquitin-protein ligase makorin-1 (MKRN1; UniProt W5PU93) and receptor of activated protein C kinase 1 (RACK1; UniProt S4TZR5) in the lung fibroblast (OAR-L1) cells (Supplementary Fig. 1c–e; Supplementary Table 3).

Since mammalian MKRN1s and RACK1s are conserved in sequence and structure (RMSD: 1.86 and 0.00, respectively; Supplementary Fig. 2a), we expressed each isoform of *Hc*-SPI-I8 as well as human RACK1 and MKRN1 in human embryonic kidney (HEK) 293 T cells and explored protein-protein interactions in a pairwise manner. We showed that both isoforms (A and B) of SPI-I8 interact with mammalian RACK1 and MKRN1 in HEK 293 T cells (Fig. 2a–c; Supplementary Fig. 2b). Consistent co-localisation and interactions were observed, irrespective of SPI-I8 isoform and mammal species (Fig. 2c; Supplementary Figs. 1e and 2b, c). Structural modelling and molecular docking suggested that a trypsin inhibitor-like domain is not required for the specific binding of SPI-I8A to mammalian RACK1 or MKRN1, but that nematode SPI-I8A/B, particularly SPI-I8B, competes with RACK1 for MKRN1 binding (Fig. 2d; Supplementary Fig. 2d). These findings indicate a role of SPI-I8 in affecting inflammatory or immune responses.

Nematode SPI-I8 inhibits host NF-κB signalling

As *Hc*-SPI-I8A/B interacts with mammalian RACK1—the negative regulator of NF-κB that mediates inflammatory responses[27,48–50]—we hypothesised that nematode SPI-I8 supresses host inflammation via the NF-κB pathway. To test this hypothesis, we first explored the relationship between RACK1 and NF-κB signalling in mammalian cells by measuring the level of the p65 protein within nuclei (Fig. 3a). It was showed that the overexpression of RACK1 significantly decreased p65 expression in both ovine (OAR-L1; $p = 0.0001$) and HEK 293 T ($p = 0.0004$) cells (Supplementary Fig. 3). Subsequently, we investigated the relationship of *Hc*-SPI-I8, RACK1 and NF-κB activity in HEK 293 T cells. Although there was no evidence that either isoform (A or B) of SPI-I8 influences *rack1* gene transcription in HEK 293 T cells (Fig. 3b), both isoforms of *Hc*-SPI-I8 decreased the transcription factor activity of NF-κB ($p = 0.0002$ for A; $p < 0.0001$ for B; Fig. 3c) as well as the abundance of the nuclear p65 protein ($p < 0.0001$; Fig. 3d, e). In particular, the non-canonical isoform of SPI-I8 (SPI-I8B) rather than the canonical isoform (SPI-I8A) was shown to induce decreased mRNA levels of the genes encoding A20 ($p = 0.0062$), IL-8 ($p = 0.0303$), IκBα ($p = 0.0014$) and TNF-α ($p = 0.2754$) (Fig. 3f–i), which accords with the effects of RACK1 in HEK 293 T cells (Fig. 3c–i). Co-expression of *Hc*-SPI-I8B and RACK1 in HEK 293 T cells led to decreased NF-κB activity ($p < 0.0001$) compared with cells expressing *Hc*-SPI-I8B alone but not compared with cells overexpressing RACK1 alone (Fig. 4a). These results imply that nematode SPI-I8 represses NF-κB cascade indirectly in mammalian cells.

Nematode SPI-I8 enhances the inhibitory activity of RACK1 in NF-κB signalling

Compared with RACK1, little is known about the role of the E3 ubiquitin protein ligase MKRN1—the other protein shown to interact with *Hc*-SPI-I8A/B in NF-κB signalling (cf. Figure 3)[51–53]. Heterologous expression of mammalian MKRN1 in HEK 293 T cells significantly increased the activity of NF-κB ($p < 0.0001$), the level of nuclear protein p65 protein ($p < 0.0001$), and the transcription of genes encoding A20 ($p = 0.0479$), IL-8 ($p = 0.0074$), IκBα ($p = 0.0018$) and TNF-α ($p = 0.1051$) in these cells (Fig. 3c–i). These results show that MKRN1, in contrast to RACK1 and SPI-I8A/B, promotes NF-κB signal transduction in HEK 293 T cells.

Although the overexpression of MKRN1 did not affect the mRNA transcription of *rack1* gene in HEK 293 T cells (Fig. 3b), it decreased the inhibitory effects of RACK1 on NF-κB activity ($p < 0.0001$; Fig. 4b), implying an MKRN1-associated negative regulation of RACK1 at the protein level. This negative regulatory effect was also observed in cells co-expressing both human MKRN1 and nematode SPI-I8B (Fig. 4c).

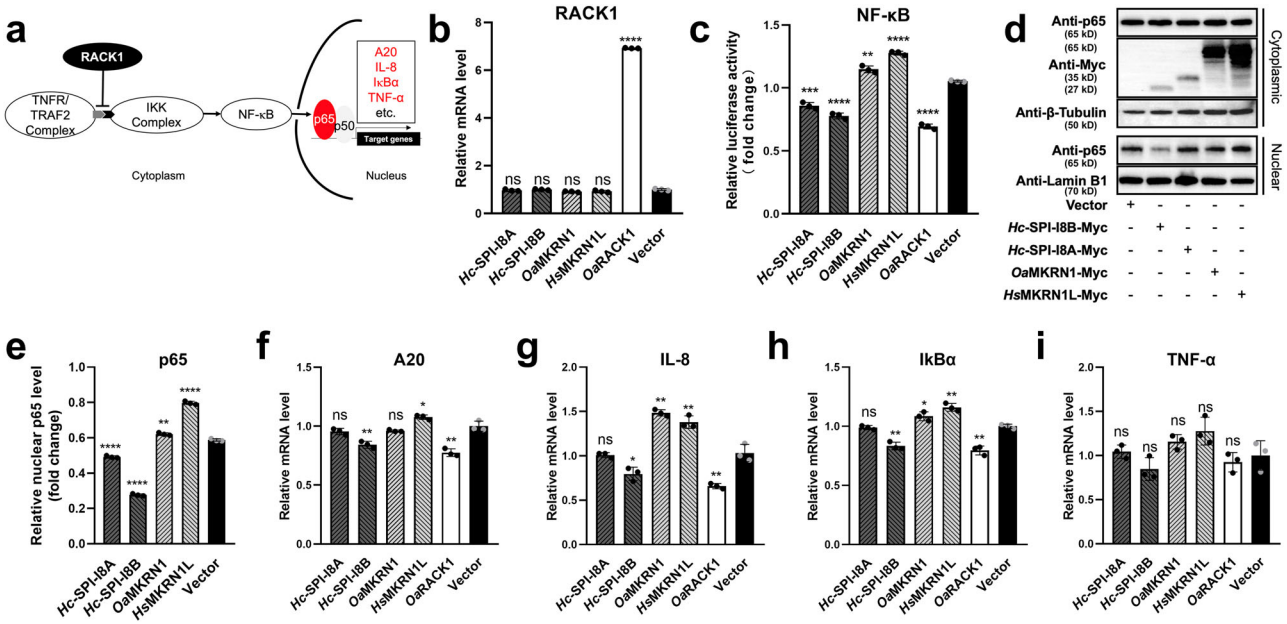

Fig. 3 | The effects of RACK1, MKRN1 and nematode SPI-I8 on NF-κB signalling in HEK 293 T cells. a Schematic diagram of NF-κB signalling cascade and the negative regulation of the TRAF2/IKKs/NF-κB signalling by RACK1. Cytoplasmic RACK1 binds IKK complex (IKKα and IKKβ), interfering with the recruitment of the IKK complex to TRAF2, which hinders the activation of NF-κB, nuclear import of p65 and subsequent transcription of downstream genes, including A20, IL-8, IκBα and TNF-α. **b** The effects of *H. contoruts* SPI-I8A/B, *Ovis aries* MKRN1, or human MKRN1 protein expression on the relative mRNA level of RACK1 in human embryo kidney (HEK) 293 T cells. **c** The effects of *H. contoruts* SPI-I8A/B, *Ovis aries* MKRN1, or human MKRN1 protein expression on the relative luciferase activity of NF-κB in HEK 293 T cells. **d**, **e** The effects of *H. contoruts* SPI-I8A/B, *Ovis aries* MKRN1, or human MKRN1 protein expression on the nuclear import of p65 in HEK293T cells, determined using western blot. **f–i** The effects of *H. contoruts* SPI-I8A/B, *Ovis aries* MKRN1, or human MKRN1 protein expression on the relative mRNA level of A20, IL-8, IκBα and TNF-α in HEK293T cells. Cells expressing *Oa*RACK1 and empty vector are used as positive and negative control, respectively. * $p < 0.05$; ** $p < 0.01$; **** $p < 0.0001$; ns, not significant.

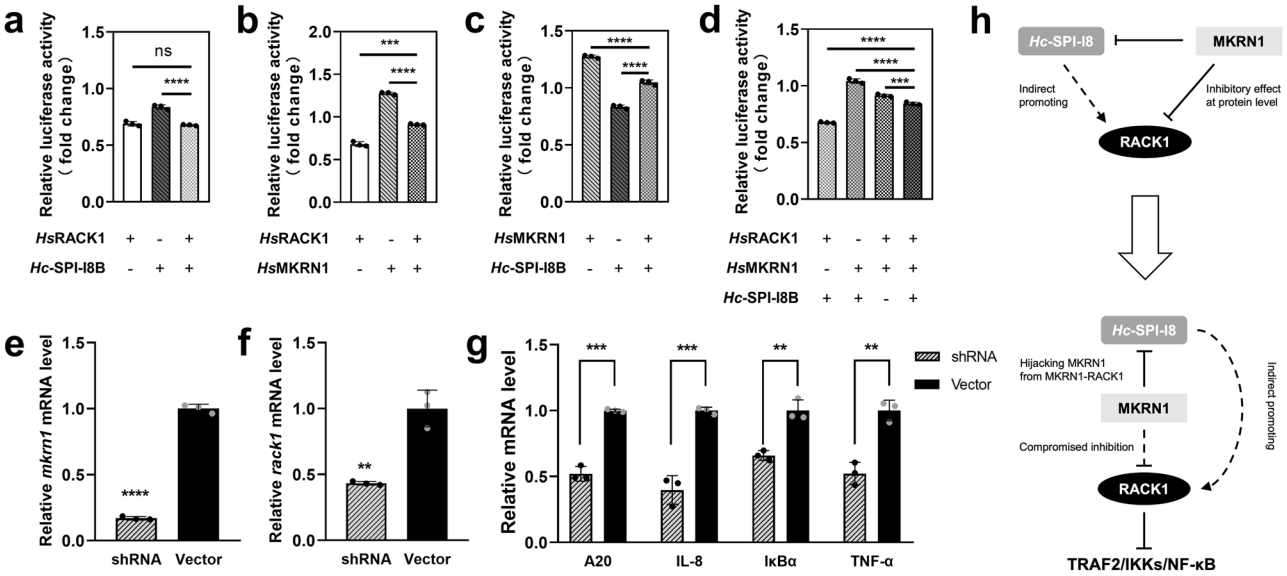

Fig. 4 | Functional relationship among nematode SPI-I8, human RACK1 and MKRN1 in HEK 293 T cells. a SPI-I8B of *Haemonchus contortus* (*Hc*-SPI-I8B) enhances the negative effect of *Hs*RACK1 on the relative luciferase activity of NF-κB in HEK 293 T cells. **b** Human MKRN1 increases the relative luciferase activity of NF-κB and abolishes the inhibitory effect of *Hs*RACK1 on NF-κB in HEK 293 T cells. **c**, **d** The promoting effect of MKRN1 on NF-κB is compromised by *Hs*RACK1 and *Hc*-SPI-I8B. **e** Lentiviral RNA interference of *Hs*MKRN1 coding gene, which **f** decreases the mRNA level of *rack1*, and **g** A20, IL-8, IκBα and TNF-α in HEK 293 T cells. **h** Schematic diagram showing the functional relationship among *Hc*-SPI-I8B, *Hs*RACK1 and *Hs*MKRN1 in HEK293T cells. *Hc*-SPI-I8 indirectly promotes the role of *Hs*RACK1 in suppressing NF-κB signalling, possibly by hijacking or interfering *Hs*MKRN1 from the *Hs*MKRN1–*Hs*RACK1 interaction. * $p < 0.05$; ** $p < 0.01$; **** $p < 0.001$; **** $p < 0.0001$; ns, not significant.

Interestingly, *Hc*-SPI-I8B relieved the MKRN1-associated suppression of RACK1 in cells expressing all three molecules (Fig. 4d). The perturbation of *mkrn1* gene transcription (Fig. 4e) significantly decreased the mRNA level of *rack1* ($p = 0.0022$) (Fig. 4f), and of genes encoding A20 ($p = 0.0001$), IL-8 ($p = 0.0007$), IκBα ($p = 0.0027$) and TNF-α ($p = 0.0020$) in RNAi-treated cells (Fig. 4g). Taken together, SPI-I8B did not increase the suppressive effect of RACK1 on NF-κB signalling, but reduced RACK1's negative regulation of, possibly by interrupting MKRN1-mediated polyubiquitination of

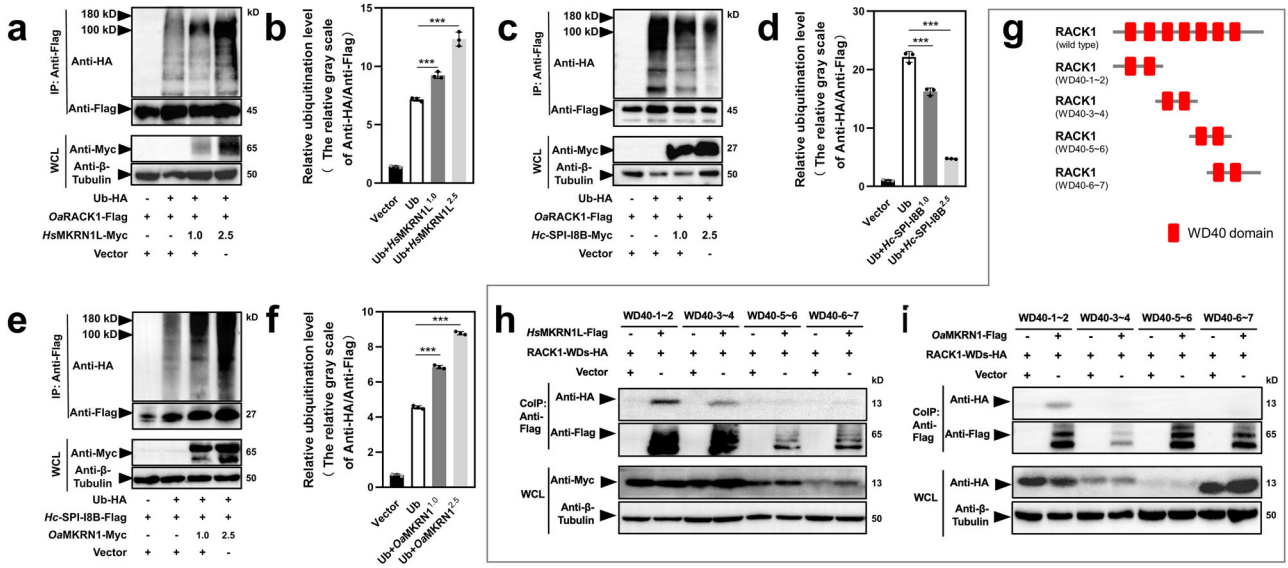

Fig. 5 | Human MKRN1-mediated polyubiquitination of RACK1 and nematode SPI-I8B in HEK 293 T cells. a The effect of *Hs*MKRN1 overexpression on RACK1 polyubiquitination is determined by immunoblot analysis, using commercial antibodies anti-HA, anti-Flag, anti-Myc and anti-β-tubulin. **b** The relative ubiquitination levels of RACK1 in HEK293T cells (gray scale of anti-HA/anti-Flag) are analysed using an Image J software (NIH Image, Bethesda, MD). Error bars are shown as mean ± standard error of mean (SEM). **c**, **d** Expression of *Haemonchus contortus* SPI-I8B decreases the relative ubiquitination level of RACK1 in HEK293T cells. **e**, **f** *Hs*MKRN1-mediated polyubiquitination of *Hc*-SPI-I8 in HEK293T cells. Tubulin or Ub is used as an internal control. *** $p < 0.001$. **g** Schematic diagram showing RACK1 domain architecture truncation strategy. WD40 domains/repeats are indicated with black blocks. **h**, **i** *Hs*MKRN1- or *Oa*MKRN1-mediated interaction of truncated RACK1 retaining the WD40-1 ~ 2, WD40-3 ~ 4, WD40-5 ~ 6, or WD40-6 ~ 7. Tubulin is used as an internal control.

RACK1 (Fig. 4h), as the RING finger domain and zinc finger motif-containing MKRN1 is a known E3 ubiquitin ligase[54,55].

Nematode SPI-I8B hijacks MKRN1-mediated polyubiquitination of RACK1

Subsequently, we assessed whether RACK1 is ubiquitinated in HEK 293 T cells overexpressing mammalian (sheep or human) MKRN1. The results showed that RACK1 is indeed ubiquitinated in a MKRN1-mediated manner (Fig. 5a, b; Supplementary Fig. 4a, b), under the influence of *Hc*-SPI-I8A/B. Surprisingly, MKRN1-mediated polyubiquitination was also detected for SPI-I8B in HEK 293 T cells (Fig. 5c–f; Supplementary Fig. 4c, d). Supported by the evidence from a three-dimensional model of the RACK1-SPI-I8-MKRN1 complex (Fig. 2d), we proposed that nematode SPI-I8 highjacks MKRN1-mediated polyubiquitination.

To test this hypothesis, we studied the region of RACK1 suggested to be involved in MKRN1–RACK1 and SPI-I8B–RACK1 interactions. Co-immunoprecipitation experiments using a truncated domain architecture of RACK1 (Fig. 5g) showed that human MKRN1 interacts with the first four WD40 repeats of RACK1 like SPI-I8B (Fig. 5h; Supplementary Fig. 5a–c), and sheep MKRN1 interacts with the first two WD40 repeats of this molecule (Fig. 5i). These findings provide experimental evidence that SPI-I8B binds to RACK1, WD40 repeats in MKRN1 (cf. Fig. 2d) and blocks RACK1 from polyubiquitination.

As lysine (K) residues are required for ubiquitination, we screened K residues that are crucial for the MKRN1-mediated polyubiquitination of RACK1. Polyubiquitination was detected on lysine residues near the fifth WD40 domain of RACK1 (Supplementary Fig. 5d–g). This region (containing K183, K185, K212 and K225) was also shown to be central to the inhibition of polyubiquitination of RACK1 by *Hc*-SPI-I8B (Supplementary Fig. 5h–k; Supplementary Fig. 6a). By mutating all these lysine residues into arginine (R) and then reverting R183/185 back to K183/185, we showed that K183 and K185 of RACK1 are essential for the polyubiquitination by human MKRN1L (Fig. 6a, b). Polyubiquitination was reduced by *Hc*-SPI-I8B on the two sites (K183 and K185) of RACK1 in HEK 293 T cells (Fig. 6c, d).

Subsequently, we determined the involvement of K48- (targeting proteins for proteasomal degradation) or K63-linked polyubiquitin chains (targeting proteins for signal production) in this process, which usually participate in proteolysis mediated by 26S proteasomes or the signal transduction[56–59]. By mutating lysine of ubiquitin at K48 to K48R or at K63 to K63R, we showed in HEK 293 T cells that human MKRN1 promotes K63-dominant polyubiquitination of RACK1 while *Hc*-SPI-I8A/B inhibits K63-dominant polyubiquitination of RACK1 (Fig. 6e–h; Supplementary Fig. 4e, f). These results reveal that MKRN1 facilitates RACK1 polyubiquitination-associated signalling (i.e. NF-κB signalling) and that nematode SPI-I8 inhibits this signal transduction.

Decreased polyubiquitination of RACK1 upregulates NF-κB signalling

Having shown that K183 and K185 residues of RACK1 are essential for the MKRN1-mediated polyubiquitination, we confirmed that these residues are also crucial for regulating NF-κB signalling in HEK 293 T cells. To do this, we mutated K183, K185, K183 or/and K185 residues of RACK1. With reference to wildtype RACK1, the mutation of all residues (lysine to arginine; RACK1-AM) resulted in a significant increase in nuclear protein p65 ($p < 0.0001$), NF-κB activity ($p = 0.0128$, $p = 0.0212$ or $p = 0.0065$), transcription levels of genes encoding A20 ($p = 0.0059$), IL-8 ($p = 0.0010$), IκBα ($p = 0.0471$) and TNF-α ($p = 0.0002$) in HEK 293 T cells (Fig. 7a–d; Supplementary Fig. 6b–d). Specifically, the mutations at K183, K185 or both K183 and K185 of RACK1 (K183R, K185R and K183R + K185R) significantly increased the nuclear abundance of p65 ($p < 0.0001$, $p < 0.0001$ and $p < 0.0001$, respectively) and the activity of NF-κB ($p = 0.0001$, $p = 0.0002$ and $p < 0.0001$, respectively) in HEK 293 T cells, compared with the non-mutated controls (Fig. 7a–d). Compared with the RACK1-AM control, the mutations at R183 or/and R185 of RACK1-AM (R183K, R185K, R183K + R185K) led to a resumption of inhibitory role on the entry of p65 protein into the nucleus, the activity of NF-κB, and the transcription of genes encoding A20, IL-8, IκBα and TNF-α in HEK 293 T cells (Fig. 7e–h). These results demonstrate that SPI-I8B protects the negative regulator RACK1 from MKRN1-mediated polyubiquitination in

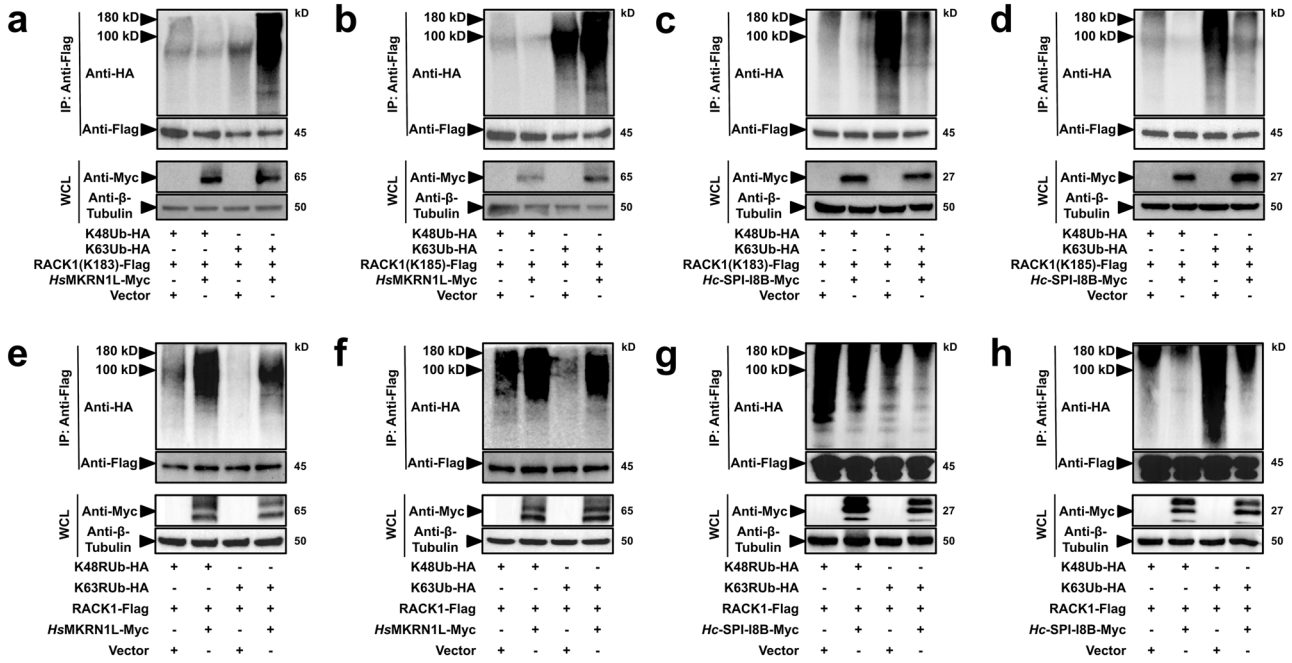

Fig. 6 | Nematode SPI-I8B decreases K63-dominant polyubiquitination at K183 and K185 of RACK1 in HEK 293 T cells. a, **b** Myc-tagged human MKRN1 mediates K48 and K63 polyubiquitination at K183 and K185 residues of Flag-tagged RACK1 in HEK 293 T cells. **c**, **d** Overexpression of *Haemonchus contortus* SPI-I8B decreased the K48 and K63 polyubiquitination at K183 and K185 residues of Flag-tagged RACK1 in HEK 293 T cells. **e**, **f** Compared with wildtype ubiquitin, site mutation of K48R and K63R of ubiquitin decreased MKRN1-mediated K48 and K63 polyubiquitination of RACK1 in HEK 293T cells. **g**, **h** Overexpression of *Hc*-SPI-I8B decreased the K48(R) and K63(R) polyubiquitination at K183 and K185 residues of Flag-tagged RACK1 in HEK 293T cells. Tubulin is used as an internal control. Cells transduced with empty vector are used as negative control.

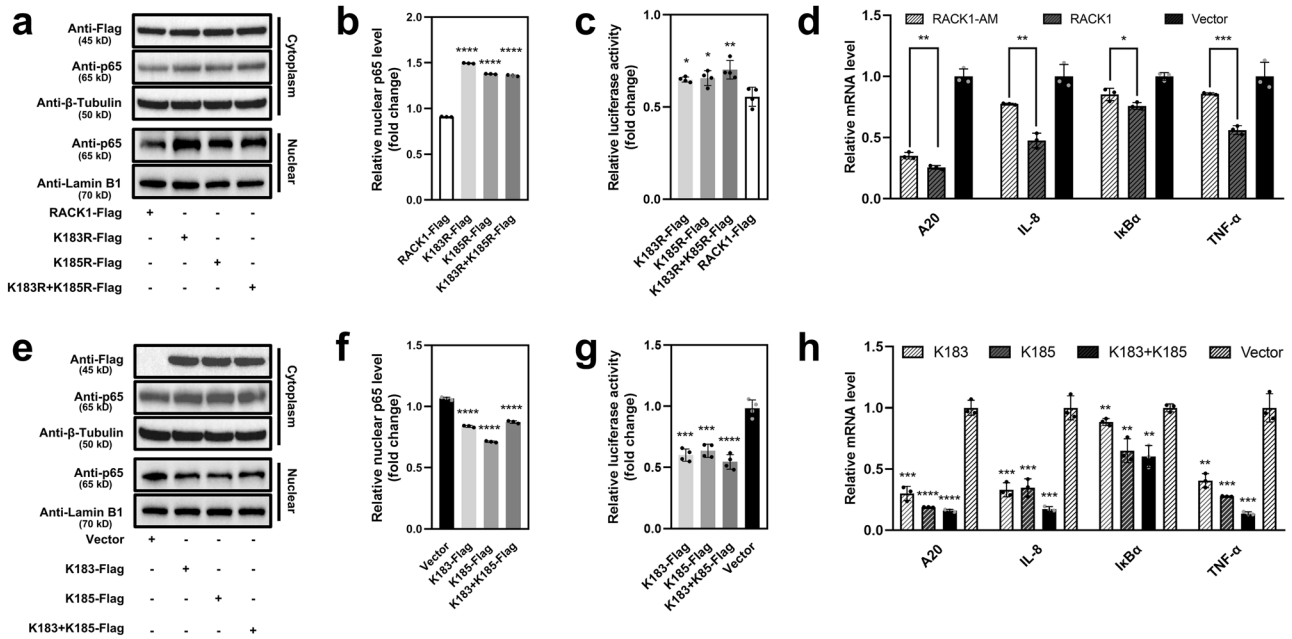

Fig. 7 | Screening of key residues involved in the polyubiquitination of RACK1. **a** Site mutation of lysine (K183 or/and K185) with arginine (K183R, K185R, or K183R + K185R) and expression of RACK1 in HEK 293T cells. **b**, **c** The influence of site mutation of RACK1 on the relative nuclear p65 level and relative luciferase activity of NF-κB in HEK 293T cells. The gray values are analysed using an Image J software. Error bars are shown as mean ± standard error of mean (SEM). **d** The influence of K183R, K185R, K212R and K225R mutations of RACK1 (RACK1-AM) on the relative mRNA levels of A20, IL-8, IκBα and TNF-α in HEK 293T cells. **e**–**h** Mutations of R183K, R185K, R212K and R225K RACK1-AM resume the negative effects of RACK1 on nuclear p65 level, NF-κB, relative mRNA levels of A20, IL-8, IκBα and TNF-α in HEK 293T cells. Cells transduced with empty vector are used as negative control. Tubulin and Lamin B1 are used as internal control of cytoplasmic and nuclear proteins, respectively. Cells transduced with empty vector are used as negative control. * $p < 0.05$; ** $p < 0.01$; **** $p < 0.001$; **** $p < 0.0001$.

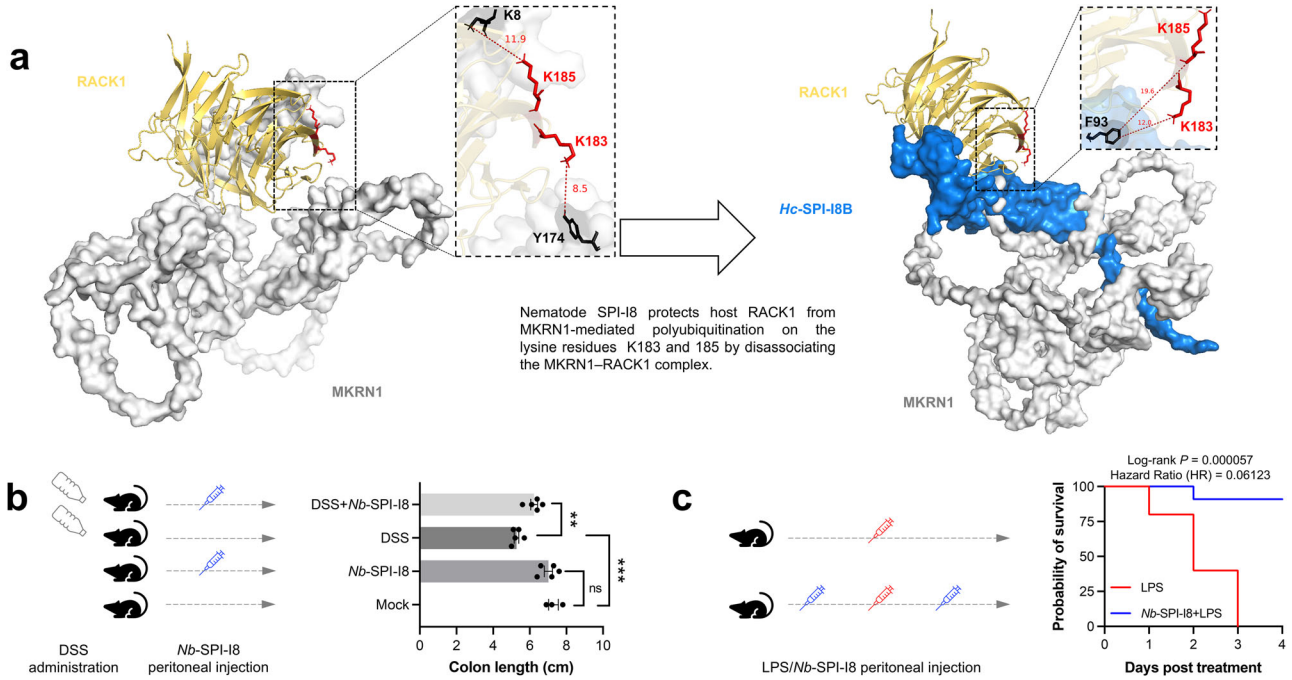

Fig. 8 | Experimental validation of the inhibitory role of nematode SPI-I8 in host inflammation. a Structural modelling and docking of MKRN1 and RACK1, *Haemonchus contortus* SPI-I8B, MKRN1 and RACK1 in silico. Nematode SPI-I8 protects RACK1 from MKRN1-mediated polyubiquitination on the lysine residues K183 and K185 by competing the space for physical interaction. K183 and K185 residues are indicated in red. The amino acid residues closest to these two residues are shown in black, and the distances has been measured. **b** Effect of recombinant *Nippostrongylus brasiliensis* SPI-I8 (r*Nb*-SPI-I8; peritoneal injection) on the colon length of mice administrated with dextran sulfate sodium (DSS)-induced colitis. Four groups were set, and five C57BL/6 mice were included in each group. The bottles indicate DSS administration through water by drinking freely. The blue injectors mean peritoneal injection of r*Nb*-SPI-I8 (50 μg per mouse). Seven days post treatment, colons of treated mice were collected and measured at autopsy. The length of each colon from mice was recorded. Student t-test analysis is used to indicate the significance of difference. ** $p < 0.01$; **** $p < 0.0001$; ns, not significant. **c** Effect of r*Nb*-SPI-I8 on the survival of mice peritoneally injected with endotoxic lipopolysaccharide (LPS)-induced systemic inflammation. Ten C57BL/6 mice were pre-treated with 50 μg SPI-I8 (the former blue injector) by intraperitoneal injection every day for three days, then treated with 150 μg SPI-I8 (the later blue injector) and 50 mg LPS (red injector) by tail vein injection on day 4. Mice (n = 10) treated with the same volume of PBS and 50 mg LPS (red injector) on day 4 to serve as positive control.

mammalian cells, supressing host NF-κB signalling and subsequent inflammation.

Nematode SPI-I8 reduces DSS-induced colitis and LPS-induced systemic inflammation in mice

Based on the predicted complex of RACK1-MKRN1, MKRN1 might promote the polyubiquitination of RACK1 through amino acid connections (K183-Y174, within 8 Å; K185-K8, within 12 Å), which was found to be changed in the RACK1-*Hc*-SPI-I8B-MKRN1 complex (K183-F93, within 12 Å; K185-F93, within 20 Å) (Fig. 8a). More complicated structure and greater distance further indicate the possibility of SPI-I8 inhibiting NF-κB signalling cascade through a mechanism of competitive inhibition. Hence, we expanded our findings that *Hc*-SPI-I8 suppresses NF-κB signalling cascade in host cells in vitro to animal experiments in vivo.

Using mouse models for inflammatory bowel disease (IBD; i.e. dextran sulfate sodium-induced colitis) and lethal sepsis (endotoxic lipopolysaccharide-induced systemic inflammation), we determined the immuno-modulatory role of SPI-I8 from another parasitic nematode *N. brasiliensis*, the hookworm of mice. Compared with controls, administration of recombinant *N. brasiliensis* SPI-I8 (*Nb*-SPI-I8; 50 μg p.i.) significantly reduced the impact of colitis on colon length ($p = 0.0026$), with no side effects detected (Fig. 8b). Additionally, treatment with recombinant *Nb*-SPI-I8 (50 μg p.i.) significantly increased the probability of survival of mice from lethal sepsis (Fig. 8c). These results show that SPI-I8 from a parasitic nematode suppresses both local and systemic inflammation and disease progression in these mouse models.

Discussion

The phylum Nematoda (nematodes) represents one of the most abundant metazoans on Earth. Extensive research has been conducted on the parasitic species, some of which are usually known by such common names as eyeworm, hookworm, lungworm, pinworm, threadworm, and whipworm, due to their medical, veterinary, and/or economic importance. Not only are these parasites interesting from a pathogenic perspective, and with these pathogens maintaining a very intricate relationship with their hosts, within that they find ways of acquiring nutrients to support their survival and development, and of neutralising direct defences from the host immune system. Effectors released by parasitic nematodes to modify host immune cells have been the subject of intensive investigation, and those present in the previously known excretory/secretory products (ESP) or recently refined extracellular vesicles represent the major repertoire of weapons to undermine the innate and acquired immune responses of humans and animals[28,29,31,60–64].

Compared with nematode infection, significant advantage would be expected in therapies using nematode effectors with immunomodulatory properties. Therefore, the use of nematodes and their effectors in treating autoimmune and allergic diseases has been proposed over the past decades[65–70]. Particularly, selected ESP molecules released by parasitic nematodes have been demonstrated to manipulate inflammation and immune responses in cell lines and in mouse models[34,71,72]. For instance, the role of a serpin secreted by *Trichinella spiralis* (pork worm) in modulating murine macrophage activation and polarisation has been tested in vitro and in vivo[73,74]. However, little is known about the action mode of a specific family of nematode protein effectors[75,76]. Clearly, a better understanding of host-parasite interactions at molecular level should underpin the research and development of "worm therapy" against inflammation- and immune-associated diseases.

On the previous studies, several helminth-derived molecules exhibit the therapeutic features in 2,4,6-trinitrobenzenesulfonic acid (TNBS)-, DSS-, or LPS-induced mice models. Grown evidence suggest the involvement of these bioactive components in suppressing type-1 or type-2 inflammation through the cyclooxygenase (COX) pathway, STAT6, p38 mitogen-activated protein kinase (MAPK), Toll-like receptor 4 (TLR4), MyD88, and NF-κB signalling[74], and multiple inflammation-related cytokines are included (i.e. TNF-α and IL-1β). However, the detailed signal transduction process remains unclear, though the helminth-derived products have been tested in treating animal inflammatory diseases. In the current work, the RACK1–TNF-α–IKKs–NF-κB axis is initially introduced into the demonstration and illustration of the mechanism underline "worm therapy" using a nematode protein (SPI-I8).

The nematode SPI-I8 studied in this work is a trypsin (a proteolytic enzyme that helps with digestion) inhibitor like molecule. Recently, we have demonstrated that the canonical form (SPI-I8A) of this inhibitor in a blood-feeding nematode plays a role in anticoagulation through interacting with a sheep TSP1 domain-containing protein using the trypsin inhibitor-like (TIL) domain, rather than exhibit a trypsin inhibitor activity[40], but had no idea about the role of the noncanonical form, a TIL domain-missing small peptide (SPI-I8B). Surprisingly, orthologs (containing a typical TIL domain) were only predicted in the Strongylida nematodes and the noncanonical isoform SPI-I8B (without TIL) was only identified in *H. contortus*. This is very likely a consequent of the draft genome assemblies and limited bioinformatic resources for most parasitic nematodes of animals, hindering genetic and functional interpretation of nematode SPI-I8 protein. Here, we report that SPI-I8, particularly the non-canonical isoform, exhibits a surprising potency in halting excessive inflammation in both an inflammatory bowel disease model (phenotype of contracted colon length) and a lethal sepsis model (phenotype of reduced survival); and elucidated a mechanism underlying this inflammation inhibition in mammalian cell lines—SPI-I8B competes a E3 ubiquitin-protein ligase (MKRN1) with a negative regulator of NF-κB signalling (i.e., RACK1[27]) in mammalian cells, protecting RACK1 from ubiquitination-mediated degradation, which suppressed inflammation initiated by NF-κB signalling. Although it has not been tested in MKRN1 and/or RACK1 knockout mice, the findings provide insights into the nature and mode of action of small serine inhibitors released by nematode in modulating host immune responses. Further investigations of these nematode effectors in aspects of delivery, absorption, distribution, metabolism, and elimination in the endogenous level are warranted. Besides, SPI-I8B that consist of disordered regions with no identifiable annotations in various widely used databases, exhibit a better potency in suppressing the NF-κB signalling pathway, which hints less relationship between the protease inhibitory activity and inflammation inhibition of SPI-I8. However, whether the unidentified elements/domains or specific sequences in SPI-I8B pose an anti-protease activity or contribute to its role in a NF-κB signalling dependent inflammation warrants further investigation. Furthermore, tuft cells have been reported to play crucial roles in mucosal immunity to gastrointestinal helminths and in colitis[36,77–79]. Investigation of the roles of nematode SPI-I8s in modulating specific immune cells like tuft cells during helminth infection should provide more information on the potential of these small serine inhibitors as host immunomodulators.

Taken together, we identified a conserved nematode small serine protease inhibitor that potently halts both local and systemic inflammation in mice models and elucidated its action mode in hijacking the poly-ubiquitination of a NF-κB signalling negative regulator. The findings provide insights into the immunomodulators of parasitic nematodes, and provide prospects for nematode therapies to relief excessive inflammation associated diseases in humans.

Materials and methods

Ethics statement

We have complied with all relevant ethical regulations for animal use. The use of sheep (*Ovis aries*, Hu sheep, male, six months old) and mice (*Mus musculus*, C57BL/6 or ICR, male, 2 weeks old) in this study was approved by the Experimental Animal Ethics Committee of Zhejiang University (permit no. 20170177 and ZJU201308-1-10-072). Blood, parasitic nematode, and abomasum were collected from naturally infected sheep by trained personnel in the Animal Hospital affiliated to the College of Animal Sciences, Zhejiang University. Handling of mice was strictly followed the Guidelines for the Use of Experimental Animals of the People's Republic of China.

Cell lines and nematodes

Ovis aries lung fibroblast (OAR-L1, cat no. IM-C034), THP-1 (cat no. IM-H260) and HEK 293 T (cat no. IM-H371) cell lines were purchased from IMMOCELL (Kunming, China), and maintained in Dulbecco's modified Eagle's medium (DMEM; Biological Industries, Beit Haemek, Israel) with 10% (v/v) foetal bovine serum (FBS; Gibco, Carlsbad, CA, USA) and Penicillin-Streptomycin (Gibco), at 37 °C and 5% CO_2 atmosphere. Eggs, L1s, L2s, L3s, L4s and adults (female and male) of *H. contortus* (ZJ strain) were prepared using a well-established method[40,76]. *N. brasiliensis* was obtained from naturally infected mouse and stored at −80 °C.

Quantitative real-time PCR (qRT-PCR)

Total RNA was extracted from worms or cells using TRIzol reagent (cat no. 15596026, ThermoFisher Scientific), and reversely transcribed into complementary DNA (cDNA) using the HiScript III 1st Strand cDNA Synthesis Kit (cat no. R312-01, Vazyme Biotechnology Ltd., Nanjing, China) in accordance with the manufacturer's instructions. DNA fragment was amplified in a 20 μL volume of the AceQ® Universal SYBR qPCR Master Mix (cat no. Q711, Vazyme Biotechnology) on a LightCycler® 480 Instrument II (Roche Diagnostics Ltd., Basel, Switzerland) following the manufacturer's instructions. All samples were analysed in triplicate. The relative mRNA levels of target genes were determined by using the $2^{-\Delta\Delta Ct}$ method[77]. β-tubulin gene was used as an internal reference for mRNA levels in *H. contortus*, and *gapdh* as the internal control in cell lines. Primer sets are shown in Supplementary Table 4.

Prokaryotic expression

Recombinant SPI-I8 of *H. contortus* (r*Hc*-SPI-I8) or *N. brasiliensis* (r*Nb*-SPI-I8) were produced in *Escherichia coli* BL21 (DE3). The coding sequence of *Hc*-SPI-I8B (without signal peptide and TIL domain) was PCR amplified from *H. contortus* cDNA and inserted into pET32a plasmids (cat no. A339132, Sangon Biotech), whereas the coding sequence of *Nb*-SPI-I8 was cloned into pET30a plasmids (cat no. B540185, Sangon Biotech). Recombinant plasmids were transformed into competent cells to express r*Hc*-SPI-I8 or r*Nb*-SPI-I8, induced by 1 mM isopropylthio-β-galactoside (IPTG) at 16 °C for 24 h. Recombinant protein was isolated from bacteria using a sonication method, then purified using Ni-NTA agarose column (cat no. 30250, Qiagen, Shanghai, China) according to the manufacturer's instructions. Purified protein was treated using a Protein Endotoxin Removal Kit (cat no. C0268, Beyotime, Shanghai, China) and quantified using a Bradford Protein Assay Kit (cat no. P0006, Beyotime) following the manufacturer's instructions. Primers used in protein expression are shown in Supplementary Table 4.

Immunohistochemistry assay

Tissue expression of SPI-I8A/B in *H. contortus* was determined by a fluorescent immunohistochemistry using a well-established method[76]. 5 μm thick sections of adult worms were prepared, blocked with 10% donkey serum (cat no. abs935, Absin, Shanghai, China), incubated with mouse anti-*Hc*-SPI-I8A/ASA polyclonal antibody (1:200) and then green fluorescein-conjugated secondary antibody (1:500; cat no. A32731, ThermoFisher Scientific). 4',6-diamidino-2-phenylindole (DAPI; cat no. D9542, Sigma-Aldrich, Shanghai, China) was used to stain the nuclei. Fluorescence was scanned using a confocal microscope (Zeiss LSM 780, Jena, Germany).

EV preparation and LC-MS/MS

Excretory/secretory products (ESP) of *H. contortus* L4 stage were obtained from culture medium[47]. EVs were further isolated from the ESP samples of

H. contortus using an ultracentrifugation method as described recently[78]. Proteins in the ESP or EVs were extracted, 150 μg of which was digested with trypsin, reduced with 10 mM dithiothreitol (DTT), alkylated with 20 mM indoleacetic acid (IAA), desalted with trifluoroacetic acid (TFA), and subjected to a Q-Exactive Orbitrap (Thermo Fisher Scientific). Peptides were identified using the Proteome Discoverer 2.1 software (Thermo Fisher Scientific).

Structural modelling and molecular docking

The 1-to-1 orthologs of *H. contortus* SPI-I8 in other parasitic nematodes were predicted and retrieved from WormBase ParaSite (WBPS18). Multiple sequence alignment of orthologous sequences was performed using the program Clustal Omega online server[79]. Structures of the nematode SPI-I8s, the ovine MKRN1 were modelled using the program AlphaFold2 v. 2.1.0[36], and human RACK1 and MKRN1 retrieved from AlphaFold Protein Structure Databas[80,81]. Molecular docking of molecules was performed using the ClusPro and HawkDock server[82–84]. Models were displayed and superimposed using UCSF ChimeraX v.1.0[85], and structural similarities between query and template sequences were measured using root-mean-square deviation (RMSD).

IP-MS

The abomasum was freshly collected from a slaughtered sheep with the contents rinsed. The inner surface tissue of the abomasum was sampled, cut into pieces (10 g/piece) and thoroughly washed with sterilized PBS. Freshly collected abomasum tissue of the naturally infected sheep was ground, filtered, and centrifuged at 3000 × g at 4 °C for cell collection. The collected cells were lysed in NP-40 lysis buffer (cat no. D9542, P0013F, Beyotime) for 0.5 h with shaking, then centrifuged at 12000 × *g* at 4 °C for supernatant collection. Coding sequence of *Hc-spi-i8* (HCON_00067680) was amplified and inserted into pcDNA3.1(+) vector (cat no. V79020, Thermo Fisher Scientific) to produce FLAG-tagged *Hc*-SPI-I8 in HEK 293 T cells. The recombinant *Hc*-SPI-I8-FLAG protein was isolated from lysed cells using anti-FLAG-conjugated magnetic beads (cat no. B26101, Bimake, Shanghai, China), and used to isolate and concentrate interactive proteins from the ovine tissue lysis. The isolated proteins were boiled, separated by sodium dodecyl sulfate-polyacrylamide gel electrophoresis (SDS-PAGE), from which proteins within a range of molecular weights from 30 to 45 kDa were subjected to digestion with trypsin (Promega), desalination with a sep-Pak C18 (Waters) and LC-MS/MS analysis with a Q-Exactive Orbitrap Mass Spectrometer (Thermo Fisher Scientific). Peptides were identified and annotated using Proteome Discoverer v.2.1.

cDNA yeast library and yeast two-hybrid screening

A cDNA library of *Ovis aries* peripheral blood mononuclear cells was constructed using the Make Your Own "Mate & Plate" Library System (cat no. 630490, Clontech, Takara Bio, USA) following the manufacturer's protocol. Total RNA was extracted from the blood-feeding L4s of *H. contortus* using TriZol reagent, reversely transcribed into the first-strand complementary DNA (cDNA), amplified by long-distance polymerase chain reaction (PCR), then processed with duplex-specific nuclease with reagents provided in the kit. Y187 yeast cells were transformed with purified nematode cDNA and pGADT7-Rec plasmids, plated onto SD/-Leu plates, and cultured at 30°C for 3–6 days, then identified with PCR.

The Matchmaker Gold Yeast Two-Hybrid System (cat no. 630489, Takara Biomedical Technology, Beijing, China) was used to identify *Hc*-SPI-8 interacting proteins, using an established method[76]. Recombinant pGBKT7 vector was used as a bait to screen the *Ovis aries* cDNA yeast library, and the selection of colonies containing interactive protein candidates was carried out by plating on to synthetic 'dropout' medium following the manufacturer's instructions. Positives were picked for sequencing and plasmid DNA extraction. The prey and bait vectors were co-transformed into Y2HGold (Takara Biomedical Technology) and then plated on to synthetic 'dropout' medium for pairwise verification.

Co-expression and co-localization

Coding sequence of genes coding for SPI-I8 (HCON_00067680), *Ovis aries* RACK1 (NP_001268408.1) or MKRN1 (XP_027824674.2), or human MKRN1 (NP_038474.2) were cloned into pLenti CMV GFP Puro (Addgene ID: 17448) or/and pLenti CMV mCherry Puro (Addgene ID: 234407). The recombinant plasmid (2 μg) was pair wisely mixed with psPAX2 (Addgene ID: 12260) and pMD2.G (Addgene ID: 12259) plasmids (2 μg) then introduced into HEK 293 T cells using polyethyleneimine (cat no. 23966, Polysciences, Warrington, PA, USA) for lentivirus packaging. The produced lentivirus was used to integrate coding sequences into the genome of OAR-L1 cells using an established method[86]. Co-localization analyses of *Hc*-SPI-I8 and *Oa*RACK1, *Hc*-SPI-I8 and *Oa*MKRN1, *Oa*RACK1 and *Oa*MKRN1 were conducted in both OAR-L1 cells and HEK 293 T cells using a confocal microscope (LSM780, Carl Zeiss). Cell nuclei were stained using DAPI (Beyotime Biotechnology).

Pull-down

The coding sequence (CDS) of *Hc*-SPI-I8A/B and *Oa*MKRN1 were inserted into pGEX-4 T-1 vector to generate recombinant plasmids which poses a GST at the N-terminal of target genes. Then, GST (as negative control) and GST-fused proteins (GST-*Hc*-SPI-I8A/B and GST-*Oa*MKRN1) were expressed via *Escherichia coli* BL21 (DE3) expression system after 1 mM IPTG inducing for 24 h at 16 °C. The induced bacteria were lysed in 50 mM PBS (pH 7.4) and the supernatant were collected after centrifugation. The WCL of HEK 293 T that overexpressed fused RACK1-HA was used as input protein. The further in vitro pull-down assay, including WCL preparation, binding, washing and subsequent blotting, was abided by our previous protocols[40] and the instructions of GST-Sefinose resins (cat no. C600031, Sangon Biotech Co., Ltd., Shanghai, China) which was used to bind GST or GST fusion proteins.

Western blot

For blotting, cells, which were harvested at least 24 h post transfecting, were lysed in NP-40 Lysis Buffer (Beyotime Biotechnology). The whole cell lysates were mixed with 5× SDS loading buffer (cat no. FD002, Hangzhou Fude Biological Technology CO., LTD., Hangzhou, China) in a dilution of 4:1 and boiled in boiling water for 10 min to prepare samples. Proteins in the samples were subsequent separated via SDS-polyacrylamide gel electrophoresis (PAGE) and transferred to polyvinylidene fluoride (PVDF) membranes (Millipore, Bedford, MA, USA), which followed by blocking in 5% (v/v) skim milk. Then the target proteins were detected on a Bio-Rad ChemiDoc Touch Imaging System (Bio-Rad Laboratories, Hercules, CA, USA) using FDbio-Femto ECL kit (cat no. FD8030, Hangzhou Fude Biological Technology) after commercial primary and secondary antibodies incubation. The primary and secondary antibodies used in this study were purchased from Cell Signaling Technology, Inc. (including HA-Tag (C29F4; cat no. 11846S), DYKDDDDK Tag (D6W5B; cat no. 15008S) and Myc-Tag (71D10; cat no. 2278S) rabbit mAb) (Danvers, MA, USA), Abways Technology (including RACK1 (cat no. CY8667), Lamin B1 (cat no. AB0054), NF-κB p65 (cat no. CY5034) Rabbit mAb) (Shanghai, China), TransGen Biotech Co., Ltd (β-Tubulin (cat no. HC101) mouse mAb) (Beijing, China), Beyotime Biotechnology (GST (cat no. AF0174) mouse mAb) (Shanghai, China) or Hangzhou Fude Biological Technology CO., LTD. (HRP AffiniPure Goat Anti-Mouse (cat no. FDM007) IgG and Anti-Rabbit (cat no. FDR007) IgG).

Co-IP

To perform Co-IP, tag protein (Myc, HA or Flag) was fused with target genes (*Hs*MKRN1S/L, *Oa*RACK1 and *Hc*-SPI-I8A/B) followed by inserting into pcDNA3.1(+) vector. EGFP, mCherry and HA was fused to the C-terminal of RACK1 to construct the recombinant plasmid based on the parental vector pLenti CMV Puro (A vector, without EGFP, which was modified from pLenti CMV GFP Puro) for generating stably transfected cell line (293 T::RACK1-EGFP, 293 T::RACK1-mCherry and 293 T::RACK1-HA). These three cell lines were separately paired with *Hs*MKRN1S/L-Flag,

*Oa*MKRN1-HA was paired with Hc-SPI-I8A/B-Flag and *Oa*RACK1-HA was respectively paired with *Hc*-SPI-I8A/B-Flag and *Oa*MKRN1-Flag for Co-IP analysis using anti-FLAG-conjugated magnetic beads (Bimake, Shanghai, China). *Hs*MKRN1L-Flag was paired with *Oa*RACK1-Myc or *Hc*-SPI-I8A/B-Myc followed by Co-IP via anti-Myc-conjugated magnetic beads (cat no. B26301, Bimake). Subsequent co-transfection, whole cellular lysates (WCL) preparation and Co-IP were carried out following the previous study and the supplier's instructions[76].

Nuclear and cytoplasmic protein extraction

For analysing the nuclear p65 protein level, the Flag tag was fused to RACK1 and its mutants, and the Myc tag was fused to *Hs*MKRN1L, *Oa*MKRN1 and *Hc*-SPI-I8A/B. The separation of nuclear and cytoplasmic proteins was performed based on the publication[87]. The HEK 293 T cells, transfected with the above vectors, were collected by centrifugation, and then washed by phosphate buffered saline (PBS) for at least three times. After several times of centrifuging and washing using 1:10 diluted NP-40 Lysis Buffer (Beyotime Biotechnology), the proteins in nuclear and cytoplasmic proteins were obtained from the sediments and supernatants, respectively. And the nuclear p65 protein level was examined through immunoblotting after sample preparation. Tubulin and Lamin B1 were used as internal control of cytoplasmic and nuclear proteins.

Luciferase reporter assay

The *Hs*MKRN1L, *Oa*MKRN1, *Hc*-SPI-I8A/B and RACK1 were respectively constructed into pcDNA3.1(+) and transfected in HEK 293 T cells, for NF-kB activity detection via luciferase reporter assays. The pNFκB-TA-luc (cat no. D2207, Beyotime Biotechnology Ltd., Shanghai, China) and Renilla luciferase pRL-TK (cat no. D2760, Beyotime Biotechnology) were used as a reporter plasmid and an internal control, respectively. About 5×10^5 HEK 293 T cells were seeded in a 24-well plate and maintained in a suitable atmosphere for 24 h. The co-transfection of reporter, control and target gene plasmids mixture were performed as above described. The cell lysates were prepared by passive lysis buffer (cat no. E1941, Promega Corporation, Madison, WI, USA) and detected using a Dual Luciferase Reporter Gene Assay Kit (cat no. 11405ES60, Yeason Biotechnology Ltd., Shanghai, China). Each transfection and testing were repeated three times.

Lentivirus-based RNA interference

Gene knockdown of *Hs*MKRN1L and *Oa*MKRN1 were performed in HEK 293 T cells with shRNAs (5'-GCGAGGGTACTGTATTTATGG-3' and 5'-GGAGCTGCCCATTTGGAGGGA-3', respectively), which were designed by BLOCK-iT RNAi Designer of Thermo Fisher Scientific (https://rnaidesigner.thermofisher.com/rnaiexpress/setOption.do?designOption=shrna&pid=8881051661280476335). Lentivirus-mediated shRNA delivery system, functioned by pLKO.1 (cat no. 8453, Addgene), psPAX2 and pMD2.G vectors, was used to knockdown the target genes according to the description of previous study[88] and the above protocols (OAR-L1 cells transduction), including virus packaging and transduction. The treated HEK 293 T cells were collected 48-72 h after plating for RNA isolation and subsequent transcriptional level analysis of target genes via RT-qPCR.

Inflammatory bowel disease model

Inflammatory bowel disease was conducted in mice by DSS[89]. C57BL/6 mice (n = 20) were randomly separated into four groups, with group 1 provided with fresh water, group 2 provided with fresh water containing 2.5% DSS (cat no. 02160110, MP Biomedicals), group 3 intraperitoneally injected with 50 μg recombinant SPI-I8, and group 4 provided with fresh water containing 2.5% DSS and injected with 50 μg recombinant SPI-I8. After seven days of treatment, the mice were sacrificed by cervical dislocation and the length of the colon of each mouse was measured at autopsy.

Lethal sepsis model

The induction of sepsis was conducted on mice by injection with LPS as described elsewhere[90]. C57BL/6 (n = 20) were separated into two groups, with group 1 pre-treated with 50 μg SPI-I8 by intraperitoneal injection every day for three days, then treated with 150 μg SPI-I8 and 50 mg LPS (cat no. L4391, Sigma-Aldrich) by tail vein injection on day 4, and group 2 treated with the same volume of PBS and 50 mg LPS on day 4. Death of treated mice were observed every 24 hours until all the mice of control group died.

Statistics and reproducibility

At least three biological or technical replicates were included, and data were presented as mean ± standard deviation (SD) or mean ± standard error of mean (SEM). The difference of relative mRNA, luciferase activity and nuclear p65 (gray value) level was analysed by Student's *t* test (comparation between two groups) or one-way analysis of variance (ANOVA) (comparation among three or more groups). $P < 0.05$ was regarded as statistically significant.

Reporting summary

Further information on research design is available in the Nature Portfolio Reporting Summary linked to this article.

Data availability

All data have been provided in the manuscript or supplementary information files (Supplementary Figs. 1–7, Supplementary Data 1/Supplementary Tables 1–4 and Supplementary Data 2). The source data in the current study are available from the corresponding author upon reasonable request. The raw data of IP-MS have been submitted to iProX (https://www.iprox.cn/page/home.html) under ProteomeXchange ID PXD055614. The newly generated plasmids in this study (pLenti CMV mCherry Puro, Addgene ID: 234407) has been deposited in Addgene.

Received: 25 August 2024; Accepted: 24 February 2025;
Published online: 03 March 2025

References

1. Scott, A. et al. What is "inflammation"? Are we ready to move beyond Celsus? *Br. J. Sports Med.* **38**, 248–249 (2004).
2. Medzhitov, R. Origin and physiological roles of inflammation. *Nature* **454**, 428–435 (2008).
3. Sorci, G. & Faivre, B. Inflammation and oxidative stress in vertebrate host-parasite systems. *Philos. Trans. R. Soc. Lond. B. Biol. Sci.* **364**, 71–83 (2009).
4. Barton, G. M. A calculated response: control of inflammation by the innate immune system. *J. Clin. Invest.* **118**, 413–420 (2008).
5. Takeuchi, O. & Akira, S. Pattern recognition receptors and inflammation. *Cell* **140**, 805–820 (2010).
6. Broom, L. J. & Kogut, M. H. Inflammation: friend or foe for animal production? *Poult. Sci.* **97**, 510–514 (2018).
7. Aqdas, M. & Sung, M. H. NF-κB dynamics in the language of immune cells. *Trends Immunol.* **44**, 32–43 (2023).
8. Levy, J. H. The human inflammatory response. *J. Cardiovasc. Pharmacol.* **27**, S31–S37 (1996).
9. Lin, C. K. & Kazmierczak, B. I. Inflammation: a double-edged sword in the response to pseudomonas aeruginosa infection. *J. Innate Immun.* **9**, 250–261 (2017).
10. Krakauer, T. Inflammasomes, autophagy, and cell death: the trinity of innate host defense against intracellular bacteria. *Mediators Inflamm.* **2019**, 2471215 (2019).
11. Rossi, J. F. et al. Dynamic immune/inflammation precision medicine: the good and the bad inflammation in infection and cancer. *Front. Immunol.* **12**, 595722 (2021).
12. Harnett, W. & Harnett, M. M. Therapeutic immunomodulators from nematode parasites. *Expert. Rev. Mol. Med.* **10**, e18 (2008).
13. Wolff, M. J. et al. Helminthic therapy: improving mucosal barrier function. *Trends Parasitol.* **28**, 187–194 (2012).
14. Wammes, L. J. et al. Helminth therapy or elimination: epidemiological, immunological, and clinical considerations. *Lancet Infect. Dis.* **14**, 1150–1162 (2014).

15. Sobotková, K. et al. Helminth therapy - from the parasite perspective. *Trends Parasitol.* **35**, 501–515 (2019).
16. Ding, J. et al. *Trichinella spiralis*: inflammation modulator. *J. Helminthol.* **94**, e193 (2020).
17. Ryan, S. M. et al. Harnessing helminth-driven immunoregulation in the search for novel therapeutic modalities. *PLoS Pathog.* **16**, e1008508 (2020).
18. Shields, V. E. & Cooper, J. Use of helminth therapy for management of ulcerative colitis and Crohn's disease: a systematic review. *Parasitology* **149**, 145–154 (2022).
19. Afonina, I. S. et al. Limiting inflammation-the negative regulation of NF-κB and the NLRP3 inflammasome. *Nat. Immunol.* **18**, 861–869 (2017).
20. Alhallaf, R. et al. The NLRP3 Inflammasome Suppresses Protective Immunity to Gastrointestinal Helminth Infection. *Cell Rep.* **23**, 1085–1098 (2018).
21. McCahill, A. et al. The RACK1 scaffold protein: a dynamic cog in cell response mechanisms. *Mol. Pharmacol.* **62**, 1261–1273 (2002).
22. Adams, D. R. et al. RACK1, a multifaceted scaffolding protein: structure and function. *Cell Commun. Signal.* **9**, 22 (2011).
23. Long, L. et al. Recruitment of phosphatase PP2A by RACK1 adaptor protein deactivates transcription factor IRF3 and limits type I interferon signaling. *Immunity* **40**, 515–529 (2014).
24. Sato, T. et al. The TRIM-FLMN protein TRIM45 directly interacts with RACK1 and negatively regulates PKC-mediated signaling pathway. *Oncogene* **34**, 1280–1291 (2015).
25. Murakami, T. et al. Cutting edge: G protein subunit β 1 negatively regulates nlrp3 inflammasome activation. *J. Immunol.* **202**, 1942–1947 (2019).
26. Wang, X. et al. Porcine RACK1 negatively regulates the infection of classical swine fever virus and the NF-κB activation in PK-15 cells. *Vet. Microbiol.* **246**, 108711 (2020).
27. Yao, F. et al. RACK1 modulates NF-κB activation by interfering with the interaction between TRAF2 and the IKK complex. *Cell Res.* **24**, 359–371 (2014).
28. Maizels, R. M. et al. Immunological modulation and evasion by helminth parasites in human populations. *Nature* **365**, 797–805 (1993).
29. Hartmann, S. & Lucius, R. Modulation of host immune responses by nematode cystatins. *Int. J. Parasitol.* **33**, 1291–1302 (2003).
30. Maizels, R. M. et al. Modulation of host immunity by helminths: the expanding repertoire of parasite effector molecules. *Immunity* **49**, 801–818 (2018).
31. Ryan, S. M. et al. Novel antiinflammatory biologics shaped by parasite-host coevolution. *Proc. Natl. Acad. Sci. USA* **119**, e2202795119 (2022).
32. Buck, A. H. et al. Exosomes secreted by nematode parasites transfer small RNAs to mammalian cells and modulate innate immunity. *Nat. Commun.* **5**, 5488 (2014).
33. Ferreira, I. B. et al. Suppression of inflammation and tissue damage by a hookworm recombinant protein in experimental colitis. *Clin. Transl. Immunol.* **6**, e157 (2017).
34. Eichenberger, R. M. et al. Hookworm secreted extracellular vesicles interact with host cells and prevent inducible colitis in mice. *Front. Immunol.* **9**, 850 (2018).
35. Buitrago, G. et al. A netrin domain-containing protein secreted by the human hookworm *Necator americanus* protects against CD4 T cell transfer colitis. *Transl. Res.* **232**, 88–102 (2021).
36. Hildersley, K. A. et al. Tuft cells increase following ovine intestinal parasite infections and define evolutionarily conserved and divergent responses. *Front. Immunol.* **12**, 781108 (2021).
37. Smyth, D. J. et al. Oral delivery of a functional algal-expressed TGF-β mimic halts colitis in a murine DSS model. *J. Biotechnol.* **340**, 1–12 (2021).
38. Loukas, A. et al. The yin and yang of human soil-transmitted helminth infections. *Int. J. Parasitol.* **51**, 1243–1253 (2021).
39. Drurey, C. et al. Intestinal epithelial tuft cell induction is negated by a murine helminth and its secreted products. *J. Exp. Med.* **219**, e20211140 (2022).
40. Wu, F. et al. The trypsin inhibitor-like domain is required for a serine protease inhibitor of *Haemonchus contortus* to inhibit host coagulation. *Int. J. Parasitol.* **51**, 1015–1026 (2021).
41. Laing, R. et al. The genome and transcriptome of *Haemonchus contortus*, a key model parasite for drug and vaccine discovery. *Genome Biol.* **14**, R88 (2013).
42. Schwarz, E. M. et al. The genome and developmental transcriptome of the strongylid nematode *Haemonchus contortus*. *Genome Biol.* **14**, R89 (2013).
43. Gasser, R. B. & von Samson-Himmelstjerna, G. *Haemonchus contortus* and Haemonchosis—Past, Present and Future Trends. *Adv. Parasitol.* **93**, 1–666 (2016).
44. International Helminth Genomes Consortium Comparative genomics of the major parasitic worms. *Nat. Genet.* **51**, 163–174 (2019).
45. Jex, A. R., Gasser, R. B. & Schwarz, E. M. Transcriptomic resources for parasitic nematodes of veterinary importance. *Trends Parasitol.* **35**, 72–84 (2019).
46. Doyle, S. R. et al. Genomic and transcriptomic variation defines the chromosome-scale assembly of *Haemonchus contortus*, a model gastrointestinal worm. *Commun. Biol.* **3**, 656 (2020).
47. Wang, T. et al. High throughput LC-MS/MS-based proteomic analysis of excretory-secretory products from short-term in vitro culture of *Haemonchus contortus*. *J. Proteom.* **204**, 103375 (2019).
48. Smith, T. F. et al. The WD repeat: a common architecture for diverse functions. *Trends Biochem. Sci.* **24**, 181–185 (1999).
49. Kiely, P. A. et al. Phosphorylation of RACK1 on tyrosine 52 by c-Abl is required for insulin-like growth factor I-mediated regulation of focal adhesion kinase. *J. Biol. Chem.* **284**, 20263–20274 (2009).
50. Nielsen, M. H. et al. Structural analysis of ribosomal RACK1 and its role in translational control. *Cell. Signal.* **35**, 272–281 (2017).
51. Gray, T. A. et al. The ancient source of a distinct gene family encoding proteins featuring RING and C(3)H zinc-finger motifs with abundant expression in developing brain and nervous system. *Genomics* **66**, 76–86 (2000).
52. Böhne, A. et al. The vertebrate makorin ubiquitin ligase gene family has been shaped by largescale duplication and retroposition from an ancestral gonad-specific, maternal-effect gene. *BMC Genomics* **11**, 721 (2010).
53. Naulé, L. & Kaiser, U. B. Evolutionary conservation of MKRN3 and other makorins and their roles in puberty initiation and endocrine functions. *Semin. Reprod. Med.* **37**, 166–173 (2019).
54. Kim, J. H. et al. Ubiquitin ligase MKRN1 modulates telomere length homeostasis through a proteolysis of hTERT. *Genes Dev.* **19**, 776–781 (2005).
55. Lee, E. W. et al. Ubiquitination and degradation of the FADD adaptor protein regulate death receptor-mediated apoptosis and necroptosis. *Nat. Commun.* **3**, 978 (2012).
56. Alkalay, I. et al. Stimulation-dependent I kappa B alpha phosphorylation marks the NF-kappaB inhibitor for degradation via the ubiquitin-proteasome pathway. *Proc. Natl. Acad. Sci. USA* **92**, 10599–10603 (1995).
57. Chen, Z. et al. Signal-induced site-specific phosphorylation targets I kappa B alpha to the ubiquitin-proteasome pathway. *Genes Dev.* **9**, 1586–1597 (1995).
58. Ben-Neriah, Y. Regulatory functions of ubiquitination in the immune system. *Nat. Immunol.* **3**, 20–26 (2002).
59. Krappmann, D. & Scheidereit, C. A pervasive role of ubiquitin conjugation in activation and termination of I kappa B kinase pathways. *EMBO Rep.* **6**, 321–326 (2005).
60. Lightowlers, M. W. & Rickard, M. D. Excretory-secretory products of helminth parasites: effects on host immune responses. *Parasitology* **96**, S123–S166 (1988).

61. Maizels, R. M. & Yazdanbakhsh, M. Immune regulation by helminth parasites: cellular and molecular mechanisms. *Nat. Rev. Immunol.* **3**, 733–744 (2003).
62. Harnett, W. Secretory products of helminth parasites as immunomodulators. *Mol. Biochem. Parasitol.* **195**, 130–136 (2014).
63. Bobardt, S. D. et al. The two faces of nematode infection: virulence and immunomodulatory molecules from nematode parasites of mammals, insects and plants. *Front. Microbiol.* **11**, 577846 (2020).
64. Okakpu, O. K. & Dillman, A. R. Review of the role of parasitic nematode excretory/secretory proteins in host immunomodulation. *J. Parasitol.* **108**, 199–208 (2022).
65. Scrivener, S. et al. Independent effects of intestinal parasite infection and domestic allergen exposure on risk of wheeze in Ethiopia: a nested case-control study. *Lancet* **358**, 1493–1499 (2001).
66. Summers, R. W. et al. *Trichuris suis* seems to be safe and possibly effective in the treatment of inflammatory bowel disease. *Am. J. Gastroenterol.* **98**, 2034–2041 (2003).
67. Summers, R. W. et al. *Trichuris suis* therapy in Crohn's disease. *Gut* **54**, 87–90 (2005).
68. Croese, J. et al. A proof of concept study establishing *Necator americanus* in Crohn's patients and reservoir donors. *Gut* **55**, 136–137 (2006).
69. Flohr, C. et al. Poor sanitation and helminth infection protect against skin sensitization in Vietnamese children: a cross-sectional study. *J. Allergy Clin. Immunol.* **118**, 1305–1311 (2006).
70. Bager, P. et al. Trichuris suis ova therapy for allergic rhinitis: a randomized, double-blind, placebo-controlled clinical trial. *J. Allergy Clin. Immunol.* **125**, 123–130 (2010).
71. Weng, M. et al. Alternatively activated macrophages in intestinal helminth infection: effects on concurrent bacterial colitis. *J. Immunol.* **179**, 4721–4731 (2007).
72. McSorley, H. J. et al. Blockade of IL-33 release and suppression of type 2 innate lymphoid cell responses by helminth secreted products in airway allergy. *Mucosal. Immunol.* **7**, 1068–1078 (2014).
73. Xu, N. et al. Recombinant trichinella pseudospiralis serine protease inhibitors alter macrophage polarization in vitro. *Front. Microbiol.* **8**, 1834 (2017).
74. Xu, N. et al. The anti-inflammatory immune response in early *Trichinella spiralis* intestinal infection depends on serine protease inhibitor-mediated alternative activation of macrophages. *J. Immunol.* **206**, 963–977 (2021).
75. Zang, X. & Maizels, R. M. Serine proteinase inhibitors from nematodes and the arms race between host and pathogen. *Trends Biochem. Sci.* **26**, 191–197 (2001).
76. Krowarsch, D. et al. Canonical protein inhibitors of serine proteases. *Cell. Mol. Life Sci.* **60**, 2427–2444 (2003).
77. Gerbe, F. et al. Intestinal epithelial tuft cells initiate type 2 mucosal immunity to helminth parasites. *Nature* **529**, 226–230 (2016).
78. Steele, S. P. et al. Tuft cells: new players in colitis. *Trends Mol. Med.* **22**, 921–924 (2016).
79. von Moltke, J. et al. Tuft-cell-derived IL-25 regulates an intestinal ILC2-epithelial response circuit. *Nature* **529**, 221–225 (2016).
80. Tunyasuvunakool, K. et al. Highly accurate protein structure prediction for the human proteome. *Nature* **596**, 590–596 (2021).
81. Varadi, M. et al. AlphaFold protein structure database: massively expanding the structural coverage of protein-sequence space with high-accuracy models. *Nucleic Acids Res.* **50**, D439–D444 (2022).
82. Comeau, S. R. et al. ClusPro: a fully automated algorithm for protein–protein docking. *Nucleic Acids Res.* **32**, W96–W99 (2004).
83. Kozakov, D. et al. The ClusPro web server for protein– protein docking. *Nat. Protoc.* **12**, 255–278 (2017).
84. Weng, G. Q. et al. HawkDock: a web server to predict and analyze the structures of protein-protein complexes based on computational docking and MM/GBSA. *Nucleic Acids Res.* **47**, W322–W330 (2019).
85. Goddard, T. D. et al. UCSF chimeraX: meeting modern challenges in visualization and analysis. *Protein Sci.* **27**, 14–25 (2018).
86. Sena-Esteves, M. & Gao, G. Production of high-titer retrovirus and lentivirus vectors. *Cold Spring Harb. Protoc.* **2018**, 273–280 (2018).
87. Jiang, M. et al. Self-recognition of an inducible host lncRNA by RIG-I feedback restricts innate immune response. *Cell* **173**, 906–919.e13 (2018).
88. Moffat, J. et al. A lentiviral RNAi library for human and mouse genes applied to an arrayed viral high-content screen. *Cell* **124**, 1283–1298 (2006).
89. Smith, P. et al. Infection with a helminth parasite prevents experimental colitis via a macrophage-mediated mechanism. *J. Immunol.* **178**, 4557–4566 (2007).
90. Bang, S. et al. Activation of GPR37 in macrophages confers protection against infection-induced sepsis and pain-like behaviour in mice. *Nat. Commun.* **12**, 1704 (2021).

Acknowledgements

We are grateful to Professor Robin B. Gasser from the Faculty of Science, The University of Melbourne for constructive comments during the drafting of this manuscript. We thank the staff in the Shared Experimental Platform for Core Instruments, College of Animal Science, Zhejiang University, and the staff from The Experimental Teaching Center, College of Animal Sciences, Zhejiang University, for their technical support. Protein structure modeling was undertaken using the LIEF HPC-GPGPU Facility hosted at the University of Melbourne. This work is funded by the National Natural Science Foundation of China (nos. 32202829, 32172877, and 32473050) and the Natural Science Foundation of Zhejiang Province (no. LQ23C180006).

Author contributions

Conceptualization—F.W. and G.M. Data curation—F.W., Y.C., and X.C. Formal analysis—Y.C., Z.D., and X.C. Funding acquisition—F.W., A.D., and G.M. Investigation—F.W., Y.C., D.T., and J.Z. Methodology—Y.Y., A.D., and G.M. Project administration—A.D. and G.M. Resources—Y.Y., A.D. and G.M. Software—F.W., Y.C., and Z.D. Supervision—A.D. and G.M. Validation—X.C. and D.T. Visualization—F.W., Z.D., and G.M. Writing—original draft preparation—F.W. writing—review & editing—C.Y., A.D., G.M.

Competing interests

The authors declare no competing interests.

Additional information

Supplementary information The online version contains supplementary material available at https://doi.org/10.1038/s42003-025-07803-8.

Correspondence and requests for materials should be addressed to Guangxu Ma.

Peer review information *Communications Biology* thanks the anonymous reviewers for their contribution to the peer review of this work. Primary Handling Editors: Dr Shitao Li and Dr Ophelia Bu.